



Stereo observations of polar stratospheric clouds

Kevin J. Mueller,^{1,2} Larry Di Girolamo,¹ Mike Fromm,³ and Steven P. Palm⁴

Received 27 February 2008; revised 1 July 2008; accepted 29 July 2008; published 10 September 2008.

[1] We present the first observations of polar stratospheric clouds (PSCs) within near-infrared (NIR) satellite images by using the Multi-angle Imaging SpectroRadiometer (MISR) to stereoscopically identify clouds with altitudes above the tropopause. Rather than using the operational MISR stereo product, a tailored stereo height algorithm operating upon MISR's most oblique viewing cameras is employed to identify PSC. Cloud top heights retrieved by this algorithm for scenes observed during the 2003 Antarctic Spring exhibit bias relative to the satellite-borne lidar, GLAS, of -0.60 ± 1.71 km for low (1–5 km altitude) tropospheric clouds, -0.35 ± 1.48 km for high (>5 km altitude) tropospheric clouds, and 0.77 ± 1.86 km for low (<18 km altitude) stratospheric clouds. During this period, MISR captured a Sep. 30th intensification of PSC spanning over 1 million sq. km and occurring as the apparent result of synoptic scale isentropic uplift associated with a potential vorticity anomaly tied to planetary waves, but likely also strengthened by a nearby tropospheric depression. **Citation:** Mueller, K. J., L. Di Girolamo, M. Fromm, and S. P. Palm (2008), Stereo observations of polar stratospheric clouds, *Geophys. Res. Lett.*, 35, L17813, doi:10.1029/2008GL033792.

1. Introduction

[2] Historically, observations of polar stratospheric clouds (PSC) have been primarily limited to those from ground-based lidar and satellite-based solar occultation instruments that suffer from poor spatial-temporal resolution and/or coverage. This, in part, has prompted a new generation of sensing instruments (e.g. satellite-based lidar) and the search for PSC analysis techniques applicable to current wide-swath high-resolution instruments. We present here a new approach, unaffected by surface or environmental temperatures, for the detection and analysis of PSC, using stereo retrievals from visible or near infrared (NIR) channel measurements captured by the Multi-angle Imaging SpectroRadiometer (MISR).

[3] The MISR instrument, launched in 1999 aboard the EOS-Terra platform, measures 446 (blue), 558 (green), 672 (red), and 866 nm (NIR) band radiance over a 360 km wide 275 m sampled swath using nine pushbroom cameras oriented with nominal viewing angles of: 70.5°, 60°, 45.6°, and 26.1° fore; 0° nadir; and 26.1°, 45.6°, 60° and 70.5° aft (respectively labeled as Df, Cf, Bf, Af, An, Aa, Ba, Ca, Da)

[Diner *et al.*, 1999]. Images of clouds within MISR's swath are sequentially captured by each of the cameras over ~6.8 minutes. Within these images, observed clouds generally produce identifiable spatial patterns of measured radiance, i.e. features. The apparent camera relative motion of such features between images, in concert with the known geometry of the cameras, allows estimation of the height and advection of clouds. This is the basis of the operational stereo cloud top height (CTH) and cloud motion vector product produced by the MISR mission since February 2000 [Diner *et al.*, 1999; Moroney *et al.*, 2002; Muller *et al.*, 2002]. Given sufficient daylight and PSC reflectivity, a stereo CTH field derived from MISR can theoretically indicate throughout the MISR swath, at 275 m horizontal resolution and 250 m precision, the presence of PSC by comparison of derived heights with estimated tropopause heights. Within this study, we find that PSC are readily discernable within MISR images. Due to the low-light sensitivity of the MISR instrument, MISR detection of PSC extends as far poleward as 85° South in September- farther than many solar occultation instruments.

[4] We demonstrate the utility of MISR in studying PSC by applying to MISR NIR band images a stereo algorithm designed for PSC detection and presented by Mueller [2008] in order to determine PSC occurrence and structure during a synoptic scale PSC intensification occurring in the early Antarctic Spring of 2003. This event was also studied by Palm *et al.* [2005] using the Geosynchronous Laser Altimeter System (GLAS), a satellite mounted lidar, which is used here as a basis for comparison.

2. Stereo Retrieval of PSC

[5] The operational MISR stereo product, hereafter labeled MSP, has been found practically incapable of retrieving PSC heights, prompting the introduction of an alternate stereo approach, hereafter labeled ALT, for determining cloud top height from MISR [Mueller, 2008]. ALT offers three key improvements upon MSP to enhance retrieval of optically thin clouds such as PSC.

[6] 1. ALT derives CTH from images captured by the far oblique cameras oriented to capture forward-scattered light (Ca and Da over Antarctica) as opposed to the near-nadir cameras (An, Af, and Aa) primarily employed by MSP. Cloud features are often more distinguishable in the former, due to increased slant path, greater reflectivity, and increased spatial contrast within the cloud [Zhao and Di Girolamo, 2004].

[7] 2. ALT employs a more robust correspondence metric than MSP. In both algorithms, regions must be identified within one image that corresponds best to some comparison region within another. However, ALT and MSP metrics of correspondence differ. In particular, the MSP metric equally weights similarities between points throughout the compar-

¹Department of Atmospheric Sciences, University of Illinois, Urbana, Illinois, USA.

²Now at Jet Propulsion Laboratory, Pasadena, California, USA.

³Naval Research Laboratory, Washington, D.C., USA.

⁴NASA Goddard Space Flight Center, Science System and Applications Inc., Greenbelt, Maryland, USA.

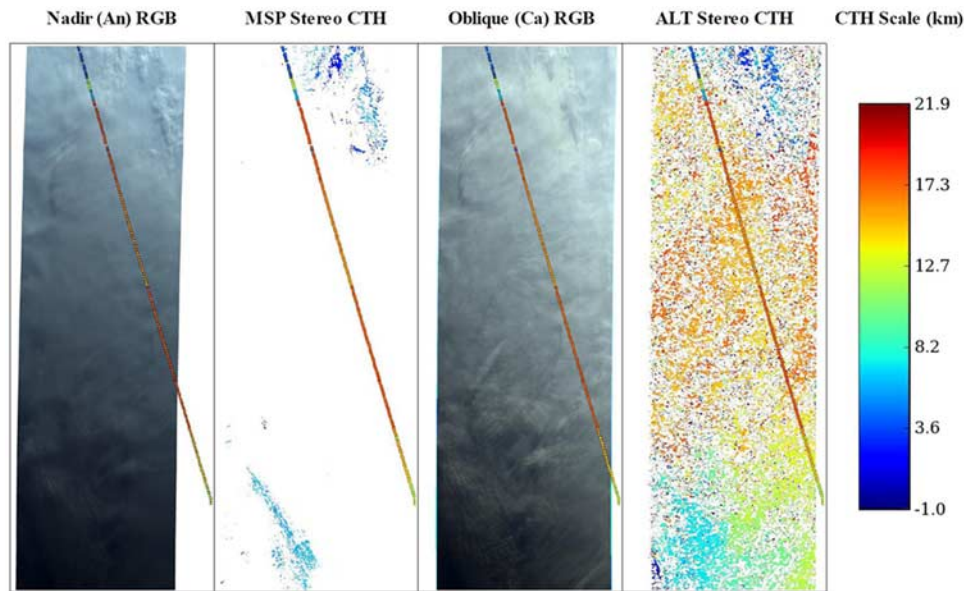


Figure 1. MSP and ALT stereo CTH retrievals with corresponding An and Ca RGB composites for MISR orbit 20125 occurring on 30 September 2003 over Queen Maudland (as mapped in Figure 2, bottom inset), projected into Space Oblique Mercator coordinates. Stereo CTH estimates are colored by height, with white representing no retrieval. Nearly coincidental GLAS lidar observed CTH estimates are also shown, using the same coloring by height, but using gray to distinguish absence of cloud.

ison regions, whereas ALT weights points at the region centers more heavily. As a result ALT stereo retrievals are theoretically more robust near depth-discontinuities such as the boundary between high altitude PSC and relatively low altitude terrain [Mueller, 2008].

[8] 3. ALT enhances the success rate of height retrieval relative to MSP, resulting in retrievals by ALT of clouds that MSP fails to identify. MSP retrievals exhibiting low correspondence are aggressively screened out to minimize noise. Due to the acknowledged imprecision of this screening [Muller *et al.*, 2002], many valid retrievals are lost. The less aggressive (and wholly different) screening of ALT allows for more retrievals, at the cost of greater noise. This noise is generally recognizable as spatially incoherent height retrievals that are often curiously dominated by values in the range from 20–30 km. (GLAS observations largely confirm that these are noise.)

[9] As a result of these three differences relative to MSP, ALT provides more numerous retrievals for all cloud heights, including those of PSC. This is exemplified by results shown in Figure 1, which were derived from MISR orbit 20125, occurring on 30 September 2003 just west of the Antarctic Plateau. Near simultaneous GLAS lidar observations collocated with this orbit demonstrate the presence within MISR’s images of a synoptic scale deck of stratospheric clouds at ~ 16 km altitude, 5 km above the tropopause. The ALT CTH retrieval is comprehensive and consistent with GLAS, whereas the MSP CTH retrieval is unavailable throughout. Figure 1 also showcases the advantages of applying stereo algorithms to the oblique camera images: cloud texture within the Ca camera image is more pronounced relative to An.

[10] Other differences between MSP and ALT reflect the depth and maturity of the operational MISR stereo product. To minimize computational load, ALT performs its matching

algorithms upon 1100 m sampled oblique NIR band images, whereas MSP operates upon a subset of 275 m resolution near-nadir red band bidirectional reflectivity values. Oblique stereo is capable of offering enhanced height resolution (250 m) versus near-nadir stereo (560 m), but ALT only delivers a precision of 1100 m. (Differences between operating upon Red versus NIR band images were not apparent.) Furthermore, unlike MSP, ALT does not correct for the influence of horizontal cloud advection occurring in the ~ 1 minute between Ca and Da views. Any advection of clouds parallel to the trajectory of MISR will be mistaken for parallax, resulting in a roughly linearly wind dependent CTH error that is constrained to within ~ 1.1 km for the estimated peak along-track wind speeds of 20 m/s present within this study.

3. Evaluation of MISR Retrieved CTH

[11] The accuracy of the ALT MISR stereo framework is evaluated through comparison of its CTH estimates with those of nearly collocated observations by the GLAS lidar. GLAS is a nadir oriented lidar carried aboard the ICESat satellite, operating at wavelengths of 532 nm and 1064 nm, and providing vertical profiles of measured cloud backscatter at 76.8 m resolution with spacing of approximately ~ 172 m along each orbit track. GLAS can measure 532 nm and 1064 nm backscatter coefficients as low as 10^{-7} 1/m-sr and 10^{-6} 1/m-sr, respectively, roughly corresponding to optical depths of 0.01 (532 nm) and 0.01 (1064 nm) [Spinhirne *et al.*, 2005]. However, the GLAS observations employed in this study have lessened sensitivity, due to a bore sighting issue (affecting only the earliest series of GLAS observations) with the 532 nm channel, and due to the exclusive use of daytime observations. Daytime lidar observations are contaminated by scattered solar radiance, more so for the 532 nm channel than the 1064 nm.

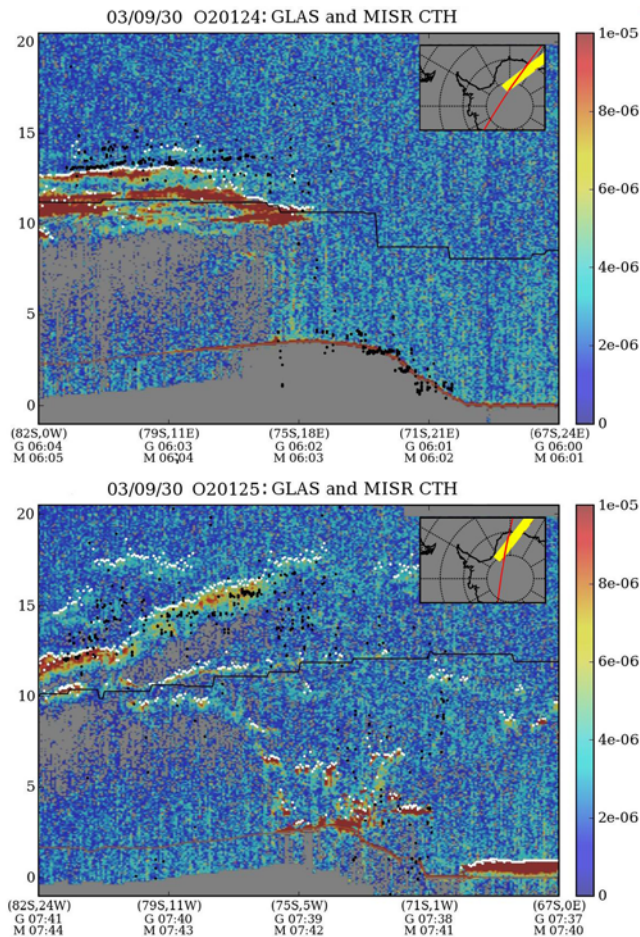


Figure 2. The track of GLAS (red curve within inset) measured vertical profiles of 1064nm attenuated backscatter ($1/\text{m}\cdot\text{sr}$) coincident with MISR orbits 20124 and 20125 (yellow swaths within inset) are plotted. MISR ALT CTH retrievals are plotted as black dots within the GLAS profile. GLAS CTH retrievals are white dots. Elevation of topography is plotted in sienna. UTC observation times by GLAS (G) and MISR (M) are labeled in addition to latitude/longitude coordinates along bottom axis. Also shown is the UKMO derived tropopause in black.

[12] Over Antarctica, during an observational period from 29 September to 12 October 2003, there were 34 MISR orbits collocated to within 10 minutes of intersecting GLAS orbits. Using these occurrences, the sensitivity and accuracy of ALT PSC height retrieval is evaluated relative to GLAS for specific cases, and over the range of data. A MISR orbit and GLAS track are considered collocated if the spatial intersection of their observations occurs within 10 minutes. A particular MISR pixel is considered collocated with any GLAS profile within a horizontal distance of 3km. Under this simple definition, a given GLAS observation might have multiple MISR pixels collocated with it, and vice-versa.

[13] A necessary component of this analysis is mitigation of noise stemming from imperfect collocation. ALT stereo height retrieval does not distinguish cloud from terrain, potentially resulting in spurious comparisons of ALT terrain height and GLAS cloud height. To minimize such noise,

only those collocated observations meeting the following criterion are compared:

[14] 1. The collocated GLAS and MISR retrieved CTH must be at least 1.0 km above the terrain (as specified by the GLA07 digital elevation model).

[15] 2. There must be a set of three or more collocated MISR CTH values within the 3 km domain associated with the GLAS observation.

[16] 3. The median CTH value within that set must be within 20% or 1.5 km of the next lowest and highest CTH values within the set.

[17] The terrain height is subtracted from all of these CTH comparisons to remove topographic effects from the analysis. Following this methodology, 2544 collocated MISR and GLAS CTH pairs are present within 34 orbits.

[18] General properties of MISR and GLAS retrievals are showcased by individual cases, including MISR orbits 20124 and 20125 shown in Figure 2. These orbits observe the apparent peak intensification of PSC associated with planetary waves and a frontal disturbance described in section 4 and by *Palm et al.* [2005]. The most notable feature of each is the strong correlation exhibited between GLAS (white dots) and ALT MISR (black dots) CTH retrievals. However, issues that influence the statistical analysis are readily apparent. Within orbit 20124, a multi-layer PSC is present with thick cirrus straddling the tropopause at ~ 11 km, an optically dense core at ~ 13 km (attenuated backscatter $\geq 1 \times 10^{-5}$), and an optically thin cloud 14 km (attenuated backscatter $\sim 4 \times 10^{-6}$). The MISR retrievals around 6° East at 14km height appear to correspond to this thin cloud, but since GLAS does not detect the cloud at that location, the comparison procedure will associate the MISR retrieval with the optically dense core below, incorrectly suggesting a positive bias to MISR retrieval. Because both MISR and GLAS produce spotty height retrieval of that apparent cloud, one might infer that MISR has similar optical depth sensitivity to GLAS. If so, this is attributable to the boresighting issue and solar contamination suffered by GLAS within these comparisons. Results from orbit 20125 showcase a different issue. When an optically thin cloud and lower altitude cloud both exist at a given coordinate, the image texture forming the basis of stereo retrieval will correspond to multiple heights. As a result, if the retrieval is successful, it may return the lower cloud height, the upper cloud height, or some average of the two. Similarly, the texture of an optically thin, geometrically thick, cloud will likely correspond to an altitude below the “true” cloud top. Either of these effects may explain MISR CTH retrievals around 16° W at 15 km, and 6° W at 13 km in orbit 20125 locations where GLAS identifies clouds existing above and below, but not level with the MISR retrieval. Other than these regions and scattered noise, the MISR CTH retrieval for the stratospheric clouds within these orbits is broadly consistent with GLAS, demonstrating the capacity of MISR to discern PSC.

[19] The 2544 MISR and GLAS CTH pairs are summarized in Figure 3 and detailed in Table S1 in the auxiliary material.¹ Results are divided into 1158 low tropospheric (1–5 km), 742 high tropospheric (5 km-tropopause),

¹Auxiliary materials are available in the HTML. doi:10.1029/2008GL033792.

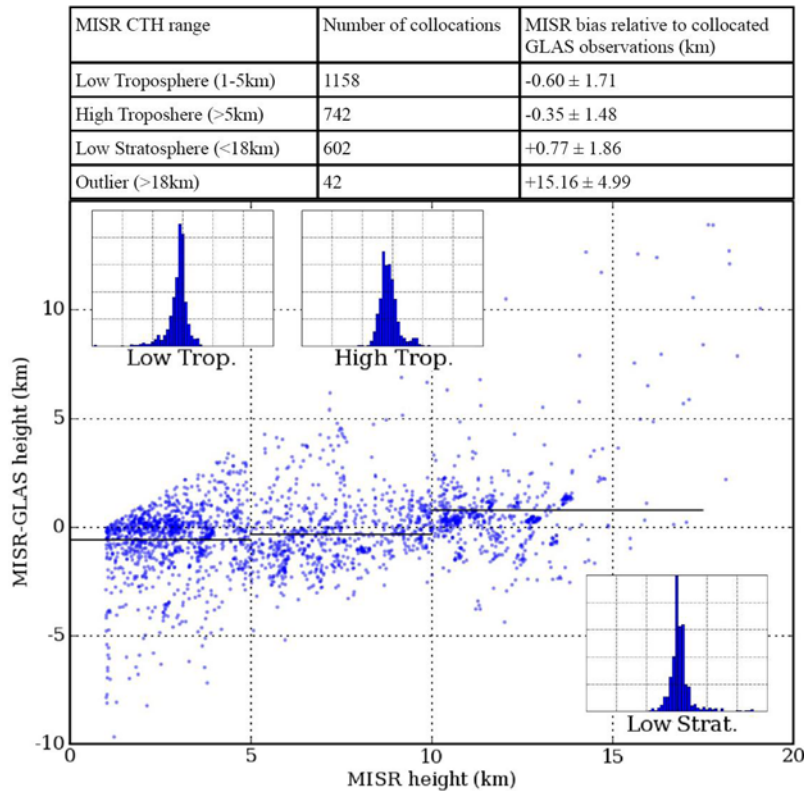


Figure 3. Statistics from coincidental GLAS and MISR CTH retrievals, scatter plotted to show height-dependent bias of MISR relative to GLAS. In the upper table, these coincidences are divided into 4 ranges for which number of observations and MISR bias is printed. Within the lower scatter plot, for 3 out of these 4 ranges, black bars representing mean bias and loosely corresponding to CTH range are plotted. Inset histograms of 0.5 km binned MISR CTH bias relative to GLAS are also shown, over a bias range from -15 km to 15 km and a frequency range from 0% to 50%.

602 low stratospheric (tropopause-18 km), and 42 outliers (18 + km) CTH retrievals. The upper bound of 18km corresponds to the highest collocated GLAS CTH recorded over the period, separating from the statistics much of the noise exhibited by the ALT stereo CTH retrieval.

[20] Multiple sources contribute to the profile of observed MISR CTH bias relative to GLAS for each CTH range. Advection of clouds by as much as 20 km (for winds of up to 20 m/s as estimated from NCEP reanalysis) during the 10 minute interval between observations can result in faulty comparisons between spatially collocated MISR and GLAS CTH retrievals corresponding to distinct clouds. Such comparisons add to the standard deviation of relative bias for all MISR retrievals, and add to (*subtract from*) the mean relative bias for MISR CTHs above (*below*) the mean GLAS height. This may, in part, explain the positive relative bias for lower stratospheric ($+0.77 \pm 1.86$ km) and negative relative bias for tropospheric ranges (-0.60 ± 1.71 km for low, -0.35 ± 1.48 km for high) of MISR CTH retrievals. Also contributing to the positive bias relative to GLAS of MISR stratospheric CTH retrievals, is the known bias of MISR ALT CTH retrieval in the presence of along-track winds. Winds aloft are predominantly westerly, with significant alternately southerly or northerly skew stemming from planetary wave structure. The along track orientation of MISR is generally southwesterly, resulting in a generally positive bias of up to 1.1 km associated with along-track winds. This positive influence on MISR CTH bias for

stratospheric retrievals may counter the negative bias contributed by the fact that MISR stereo retrieval does not necessarily resolve the cloud “top”, but, rather, the location of the cloud producing the most contrast within images. This location resides at or below the top to an extent not well characterized.

4. Antarctic PSC Intensification of 30 September 2003

[21] *Palm et al.* [2005] introduced and analyzed an intensification of PSC appearing first over the Weddel Sea and then over the Antarctic plateau within observations from numerous GLAS orbits covering a period from 29 September to 1 October 2003. Development of the apparently contiguous PSC deck observed by GLAS was attributed to cooling associated with planetary wave activity, although extensive tropospheric cloudiness was also observed and taken to suggest the involvement of a tropospheric disturbance. This latter interpretation is also supported by the spatial-temporal correlation of PSC development with cyclogenesis observed by MISR and shown in Figure 4 (and also in Animation S1 in the auxiliary material), which maps snapshots of ALT stereo derived cloud structure and altitude for each day from 27 September to 1 October. This cyclogenesis is showcased and labeled within Figure 4 by white stars denoting: vortex development on 29 September indicated by a slot of clear air within a hook-shaped cloud deck; and full vortex maturity on

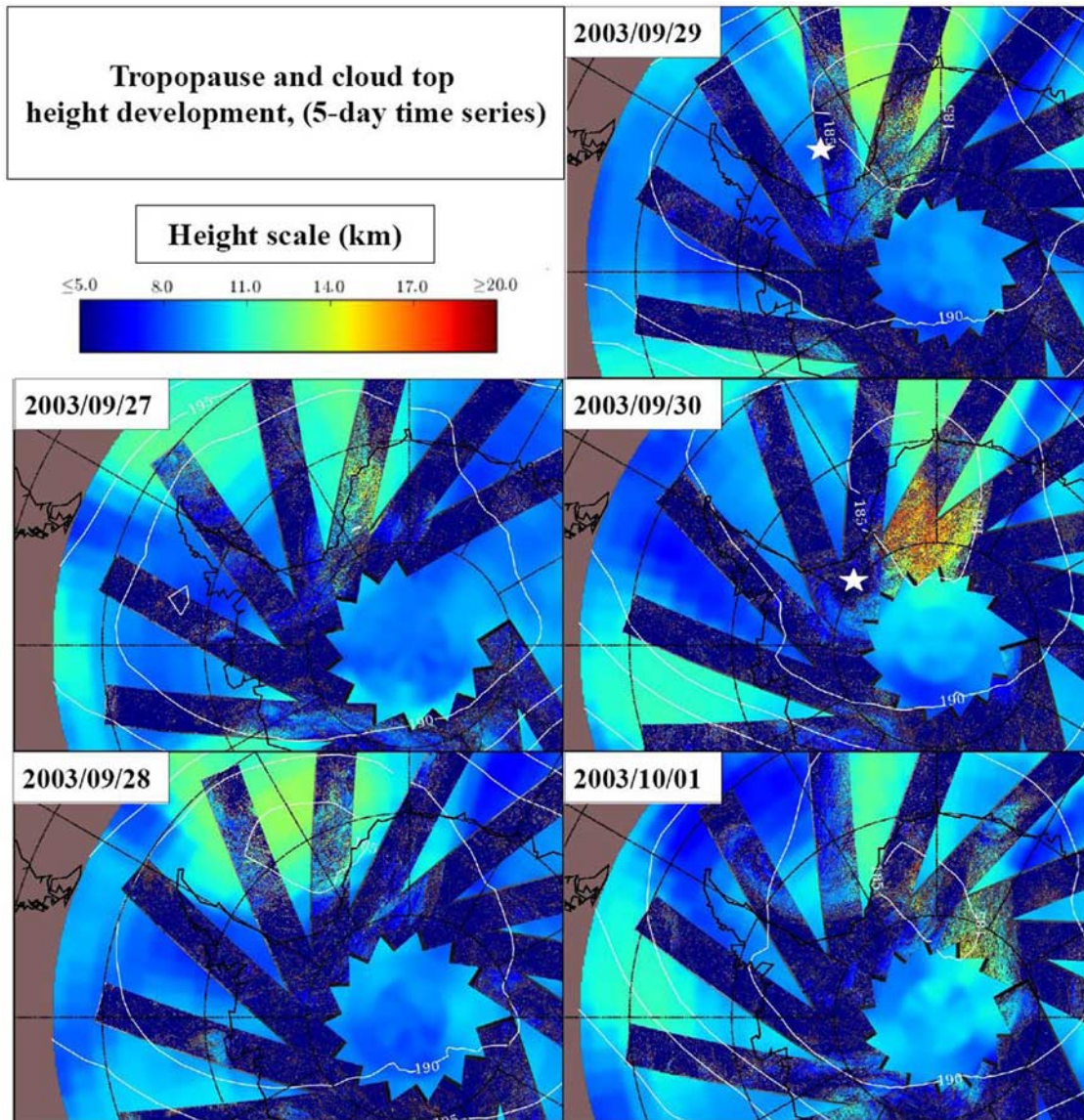


Figure 4. Time series of ALT stereo CTH retrievals over Antarctica from 27 September to 2 October 2003. The altitude color scale at upper left also applies to UKMO derived tropopause heights mapped in the background of each day's plot, allowing ready identification of 18 km PSC (tinted dark orange) relative to the tropopause, which peaks at 13 km (tinted aqua). UKMO temperature contours are also shown.

30 September indicated by a center into which alternating bands of clear air and cloud spiral. Both MISR and GLAS observations show an unbroken progression of cloud altitude from lower troposphere to stratosphere on 30 September, with MISR more clearly showing that this progression of cloud height spirals out from the vortex eye to the outermost vortex band. UKMO meteorological analysis of tropopause height from isentropic potential vorticity (IPV) (i.e. the height where IPV equals -3PVU) and minimum stratospheric temperature shows that PSC (identified as cloud altitudes above the tropopause) appeared at the outermost vortex band within a cold pool associated with an upper tropospheric-lower stratospheric (UTLS) IPV anomaly (identified as a region of increased tropopause height). This IPV anomaly, weakly present on 27 September and having likely origins in planetary wave

structure, strengthens considerably on 28 September, forcing ascent and adiabatic cooling of air parcels advected along sloping isentropes resulting in cooling as described by *Teitelbaum et al.* [2001]. The clear 29 September signal of vortex development suggests that cyclogenesis also began on 28 September, induced by and then strengthening the IPV anomaly until 30 September when both the vortex and anomaly show decay. Throughout the lifetime of the UTLS IPV anomaly, the lower stratosphere cooled, ultimately producing a synoptic pool of cold air at temperatures below the stratospheric frost point ($\sim 185\text{ K}$), within which high backscatter ratio (as detected by GLAS) PSC appeared in abundance on 29 September and covered a maximum extent of at least $\sim 10^6\text{ km}^2$ on 30 September.

[22] In addition to cloud height and extent, MISR NIR (and visible) band observations also allow inspection of

cloud texture (shown in the auxiliary material). During this event, there were two distinct textures of stratospheric cloud: one cirrostratus-like, located along and directed parallel to the eastern edge of the outermost vortex band; and the other cirrocumulus-like, existing at higher altitudes and located along the western interior of the outermost vortex band. These different textures could indicate differences in type and/or life cycle of PSC, or, more simply, could reflect the strength of surrounding winds.

5. Conclusions

[23] A stereo technique applied to MISR NIR band images captured over the poles has been developed in order to provide high-resolution examination of PSC structure and frequency with expansive per day coverage available year round for sunlit polar regions. Principally differing from previous stereo techniques by the correspondence metric and by the use of oblique camera pairs, the technique, labeled ALT, was found to return far more retrievals, especially for PSC, which the standard MISR stereo product often fails to detect. To evaluate the ALT technique, 2544 MISR CTH retrievals were analyzed, each within 10 minutes and ~ 3 km of a GLAS lidar retrieval. Relative to GLAS, MISR was found to exhibit a bias of -0.60 ± 1.71 km for low (1–5 km altitude) tropospheric clouds, -0.35 ± 1.48 km for high (>5 km altitude) tropospheric clouds, and 0.77 ± 1.86 km for low (<18 km altitude) stratospheric clouds.

[24] ALT stereo retrievals were used to analyze an intensification of PSC occurring in the early Antarctic spring of 2003, 27 September to 1 October. Stereo observations confirmed by GLAS measurements throughout the period, in conjunction with UKMO reanalysis, suggest that the PSC developed from an isentropic potential vorticity anomaly associated with planetary waves and strengthened by tropospheric cyclogenesis. These findings show the potential value of two-dimensionally resolving horizontal

PSC structure at 275 m resolution. Dating back to 2000, MISR's ongoing observational record provides a unique capacity: to not only expose relationships between sunlit PSC structure and frequency, mesoscale weather, and internal gravity waves; but also to determine interannual trends in sunlit PSC behavior.

References

- Diner, D. J., R. Davies, L. Di Girolamo, Á. Horváth, C. Moroney, J. P. Muller, S. Paradise, D. Wenkert, and J. Zong (1999), MISR level 2 cloud detection and classification algorithm theoretical basis document, *JPL Tech. Doc. D-11399*, Jet Propul. Lab., Calif. Inst. of Technol., Pasadena.
- Moroney, C., R. Davies, and J.-P. Muller (2002), Operational retrieval of cloud-top heights using MISR data, *IEEE Trans. Geosci. Remote Sens.*, *40*, 1532–1540.
- Mueller, K. J. (2008), Stereo observations of polar stratospheric clouds, M. S. thesis, Univ. of Ill., Urbana.
- Muller, J. P., A. Mandanayake, C. Moroney, R. Davies, D. J. Diner, and S. Paradise (2002), MISR stereoscopic image matchers: Techniques and results, *IEEE Trans. Geosci. Remote Sens.*, *40*, 1547–1559.
- Palm, S. P., M. Fromm, and J. Spinhrne (2005), Observations of antarctic polar stratospheric clouds by the Geoscience Laser Altimeter System (GLAS), *Geophys. Res. Lett.*, *32*, L22S04, doi:10.1029/2005GL023524.
- Spinhrne, J. D., S. P. Palm, W. D. Hart, D. L. Hlavka, and E. J. Welton (2005), Cloud and aerosol measurements from GLAS: Overview and initial results, *Geophys. Res. Lett.*, *32*, L22S03, doi:10.1029/2005GL023507.
- Teitelbaum, H., M. Moustouai, and M. Fromm (2001), Exploring polar stratospheric cloud and ozone minihole formation: The primary importance of synoptic-scale flow perturbations, *J. Geophys. Res.*, *106*, 28,173–28,188.
- Zhao, G., and L. Di Girolamo (2004), A cloud fraction versus view angle technique for automatic in-scene evaluation of the MISR cloud mask, *J. Appl. Meteorol.*, *43*, 860–869.
- L. Di Girolamo, Department of Atmospheric Sciences, University of Illinois, 105 South Gregory, Urbana, IL 61801, USA.
- M. Fromm, Naval Research Laboratory, Code 7227, Washington, DC 20375-0001, USA.
- K. J. Mueller, Jet Propulsion Laboratory, 4800 Oak Grove Drive M/S T1721, Pasadena, CA 91109, USA. (kmueller@jpl.nasa.gov)
- S. P. Palm, NASA Goddard Space Flight Center, Science Systems and Applications Inc., Code 613.1, Greenbelt, MD 20771, USA.